Magnetism of Leaves of Azalea
—— Characters and Correlation with the Environment ——

Naoko UENO

東洋大学紀要　自然科学篇　第51号　抜刷

Reprinted from

Journal of Toyo University, Natural Science
No.51, pp.99～119, March, 2007
Tokyo, Japan

Magnetism of Leaves of Azalea
—— Characters and Correlation with the Environment ——

Naoko UENO*

Abstract

NRM (natural remanent magnetism) of leaves of azalea varies with the sampling point from $2x10^{-6}(Am^2/kg)$ to $83x10^{-6}(Am^2/kg)$, reflecting the declination of the geomagnetic field of the earth. IRM (isothermal remanent magnetism) saturates at 250-300mT. SIRM (saturated IRM) varies from $60x10^{-6}(Am^2/kg)$ to $3400x10^{-6}(Am^2/kg)$. Susceptibility ranges from $0.1x10^{-8}m^3/kg$ to $26.9x10^{-8}$ m^3/kg. The largest NRM, SIRM and susceptibility are acquired from the leaves near the platform of the railway station and the smallest are from Matsumoto city in the snow season. NRM, SIRM and susceptibility from the crowded road in Tokyo are higher than those from the suburbs. The reason of the high intensities is considered as the enrichment of the magnetic dust in the air around the sampling site. Leaves of azalea have cilia and are sticky to catch and keep and absorb the dust in the air. The hysteresis analysis shows Jrs/Js varies from 0.2 to 0.3, Hc varies from 14 mT to 22 mT, and Hcr varies from 33 mT to 66 mT respectively. These hysteresis parameters suggest that the main magnetic mineral is psudo-single domain magnetite. In X-ray diffraction analysis of magnetic powder (attractive to magnets) under 180μm, Ankerite ($Ca(FeMg)(CO_3)_2$) is suggested as the Fe containing mineral with the low reliability. In SEM-EDX analysis, particles containing Fe oxide, metallic Fe and Fe included in silicate are identified qualitatively. In the Mössbauer effect analysis, magnetite could not be found and β-FeO(OH) and γ-FeO(OH) are suggested to the main magnetic minerals. Total Fe content of natural leaves is 0.053% according to the wet chemical analysis, and is 0.13% of the dried powder leaves.

Key words: magnetizm of leaves, azalea

* 上野直子：東洋大学文学部　〒 112-8606　東京都文京区白山 5-28-20
Faculty of Literature, Toyo University, 5-28-20, Hakusan, Bunkyoku, Tokyo 112-8606 Japan

1. Introduction

Natural remanent magnetizm (NRM) of plants was studied on various kinds of vegetables and leaves (Ueno, 1993), especially that of kiku (compositae) (Ueno, 1996). These reports show that the NRM of kiku is strong and stable, and reflects the declination of the geomagnetic field. After the reports, the author found that NRM of the leaves of the azalea was stronger than kiku (Ueno, 1997).

Azalea is the most familiar roadside tree in Japan, and the leaves are with thin hair on both sides of the surface and sticky when handled with fingers. In this report, results of the experiments on leaves of azalea about initial susceptibility, alternated field (AF) demagnetization of NRM, SIRM and orthogonal IRMs,hysteresis parameters, X-ray diffraction analysis, SEM-EDX analysis, wet chemical analysis of Fe content, Mössbauer effects analysis, and microscopic observations are reported.

2. Sample Preparation

Samples were collected mainly in Tokyo, from azales near railway stations, in the town including the roadside and in the suburbs of Tokyo such as Asaka city, Hayama town and Kurihama town. Besides Tokyo area, leaves were collected from Matsumoto city in the central Japan and Kagoshima city in Kyushu (Fig.1). Sample numbers (No.), classification, locality and abbreviation of the sample are listed in Table.1.

For the rock magnetic experiments, leaves were collected of which direction of the veins were directed nearly to the north of the geo-magnetic field. Piled leaves were cut to fit the sample case as illustrated in Fig.2.

3. Experiment and results

In Fig.3, four examples of the results of NRM, SIRM and IRM measurements are shown. Sample (No.5) shown in Fig.3-1 was collected from the railway station, No.14 in Fig.3-2 was from near the rail, No.30 in Fig. 3-3 was from Kagoshima city and No.42 in Fig.3-4 was collected from Matsumoto city.

(1) NRM: NRM was measured using SQUID at NIPR (National Institute for Polar Research). Data varies from $2x10^{-6}$ Am^2/kg to $83x10^{-6}$ Am^2/kg (Table.1). The largest value was obtained from the leaves at the railway stations, while the lowest one was from that in Matsumoto city situated at the countryside. Mean AF (alternating field) demagnetization field (MDF, showing the half NRM) ranges from 35 mT to 40mT (Fig.3). Zijderbelt diagram that shows the directional change during AF demagnetization is also shown in Fig.3. Leaves from Kagoshima city collected soon after the ash fall of the Sakurajima volcano are characterized by the small NRM and large SIRM.

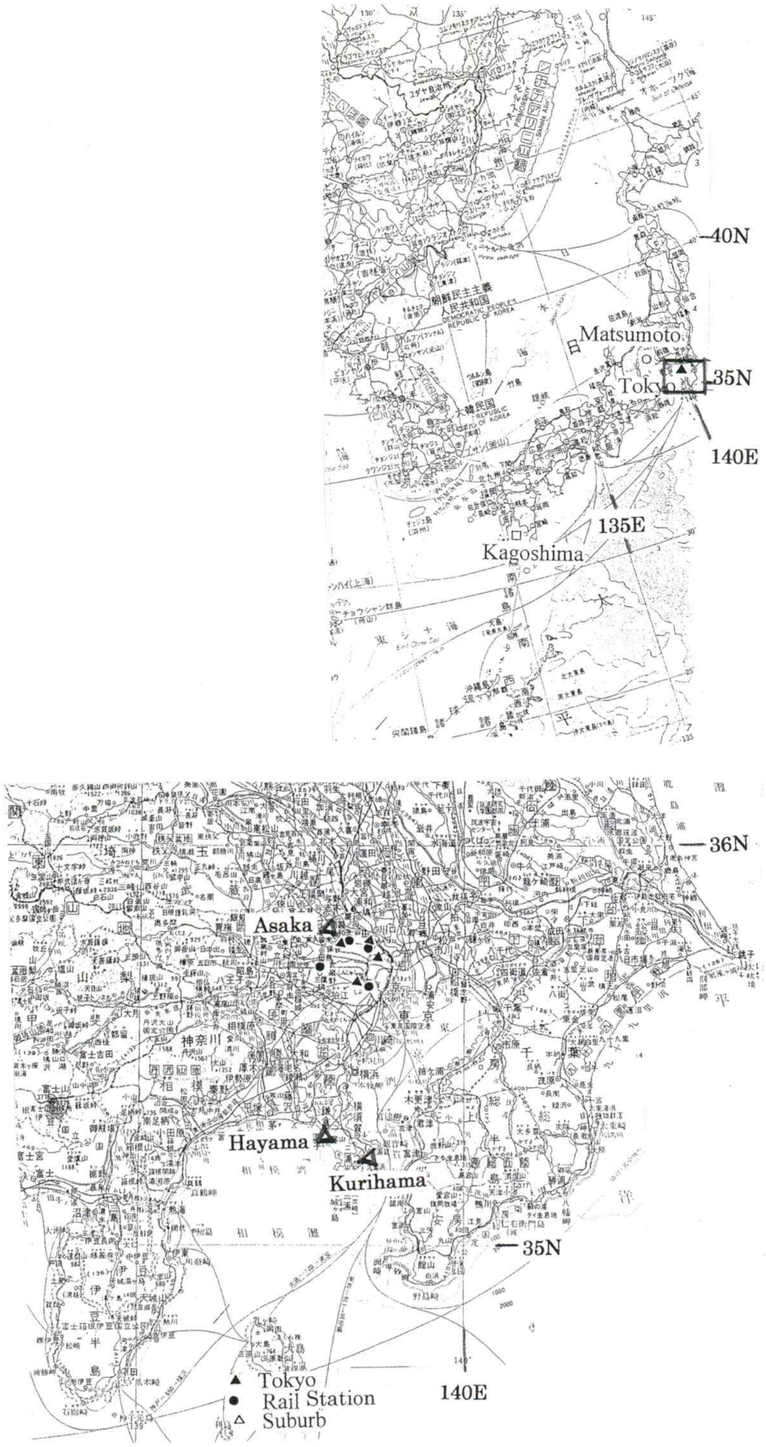

Fig. 1.
Maps of the sampling sites

	sample No.	site	NRM ($10^{-6}Am^2/kg$)	SIRM ($10^{-6}Am^2/kg$)	X ($10^{-8}m^3/kg$)	SIRM/X ($10^2A./m$)	SIRM/NRM	採取場所
●	1	Shinoakatsuka Stn	49.7	3401	26.9	126	68.4	下赤塚駅
●	2	Shimoitabashi Stn	82.9	2743	15.9	173	33.1	下板橋駅
●	3	Shimoitabashi Stn	37.3	2720	20.1	135	72.9	下板橋駅
●	4	Shimoitabashi Stn	19.4	2130	12.6	169	109.8	下板橋駅
●	5	Harajuku Stn	18.1	2094	22.2	94	115.7	原宿駅
●	6	Harajuku Stn	5.6	548	6.6	83	97.9	原宿駅
●	7	Harajuku Stn	17.6	1550	20.2	77	88.1	原宿駅
●	8	Mitaka Stn	39.8	849	16.0	53	21.3	三鷹駅
●	9	Shimoitabashi Rail	31.5	1616	21.1	77	51.3	下板橋駅踏切
●	10	Near Narimasu Stn	21.1	1585	10.3	154	75.1	成増駅踏切
●	11	Near Narimasu Stn	16.7	1387	9.3	149	83.1	成増駅踏切
●	12	Near Narimasu Stn	19.4	1280	11.5	111	66.0	成増駅踏切
●	13	Near Tokumaru	15.1	665	5.5	121	44.0	徳丸線路際
●	14	Near Akatsuka	12.6	440	2.7	163	34.9	赤塚線路際
●	15	Near Takatanobaba Stn	7.2	340	5.5	62	47.2	高田馬場駅前
●	16	Near Shimoitabashi Stn	3.8	390	3.8	103	102.6	下板橋駅前
●	17	Near Shimoitabashi Stn	9.1	351	4.8	73	38.4	下板橋駅前
●	18	Near Shimoitabashi Stn	12.4	579	5.5	105	46.7	下板橋駅前
▲	19	Hakusan Toyo	16.6	541	7.7	70	32.6	白山東洋大前
▲	20	Hakusan-ue	23.0	766	10.5	73	33.3	白山上
▲	21	Hakusan-ue	34.4	1005	18.3	55	29.2	白山上
▲	22	Itabashi-kuyakusyo-mae	14.2	653	12.4	53	46.0	板橋区役所前
▲	23	Yoyogi Park	3.1	172	2.0	86	55.5	代々木公園
▲	24	Akatsuka Kawagoe-road	7.5	238	3.3	72	31.7	赤塚川越街道
▲	25	Akatsuka Kawagoe-road	10.5	467	6.3	74	44.5	赤塚川越街道
▲	26	Akatsuka Kawagoe-road	9.4	315	3.2	98	33.5	赤塚川越街道
▲	27	Akatsuka Kawagoe-road	7.0	143	3.5	41	20.4	赤塚川越街道
□	28	Kagoshima Univ	5.8	1371	5.0	272	236.4	鹿児島大
□	29	Kagoshima Univ	4.7	1221	7.0	174	259.8	鹿児島大
□	30	Kagoshima Univ	5.5	523	2.5	209	95.1	鹿児島大
□	31	Matsubata town	6.8	1426	9.6	149	209.7	松原町
□	32	Matsubata town	5.9	1188	8.2	145	201.4	松原町
□	33	Nakagori Town	10.3	1300	8.1	160	126.2	中郡町
□	34	Nakagori Town	12.2	1165	7.4	157	95.5	中郡町
△	35	Asaka Toyo	12.6	451	5.3	85	35.8	朝霞東洋大
△	36	Asaka Toyo	5.8	325	4.5	72	56.0	朝霞東洋大
△	37	Asaka Toyo	11.2	553	7.0	79	49.4	朝霞東洋大
△	38	Hayama town	5.0	157	2.6	60	31.4	葉山町
△	39	Kurihama town	13.5	467	5.4	86	34.6	久里浜
○	40	Matsumoto Castle	2.7	91	2.0	45	33.7	松本城
○	41	Matsumoto City Office	1.8	80	0.9	89	44.4	松本市役所
○	42	Shinsyu Univ	1.9	57	1.9	30	30.0	信州大
+	43	Kagoshima Univ(wash)	5.5	903	7.5	120	164.2	鹿大(水洗浄)
+	44	Shimoitabashi Stn(wash)	13.3	741	6.6	112	55.7	下板橋駅(超音波洗浄)

● near the railway ▲ crowded city □ Kagoshima
△ Suburbs ○ Matsumoto + Others

Table 1.
Sample description and Intensity of NRM, SIRM, χ

Fig.2.
Procedures of the sample preparation and sampling site of No.2

No.5 Harajuku ●

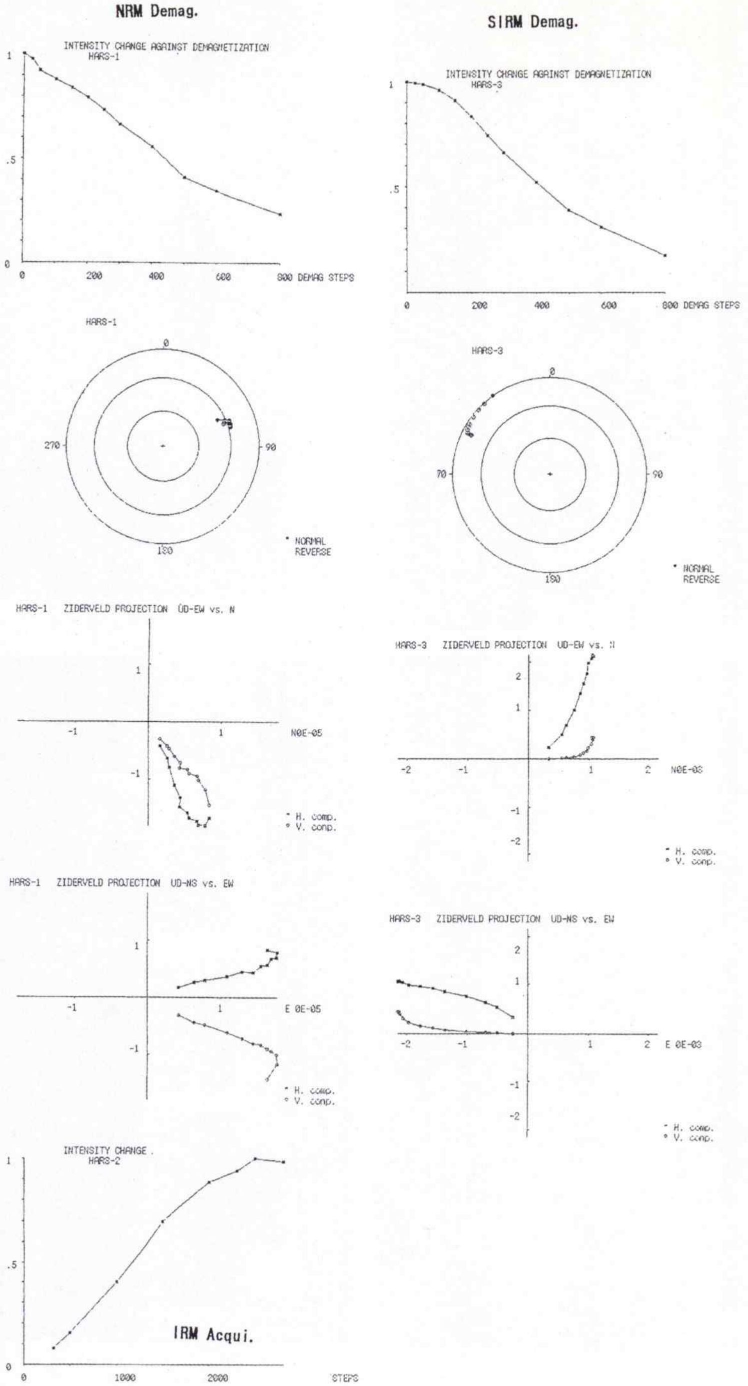

Fig.3-1.
Sample No.5

No.14 Akatsuka ●

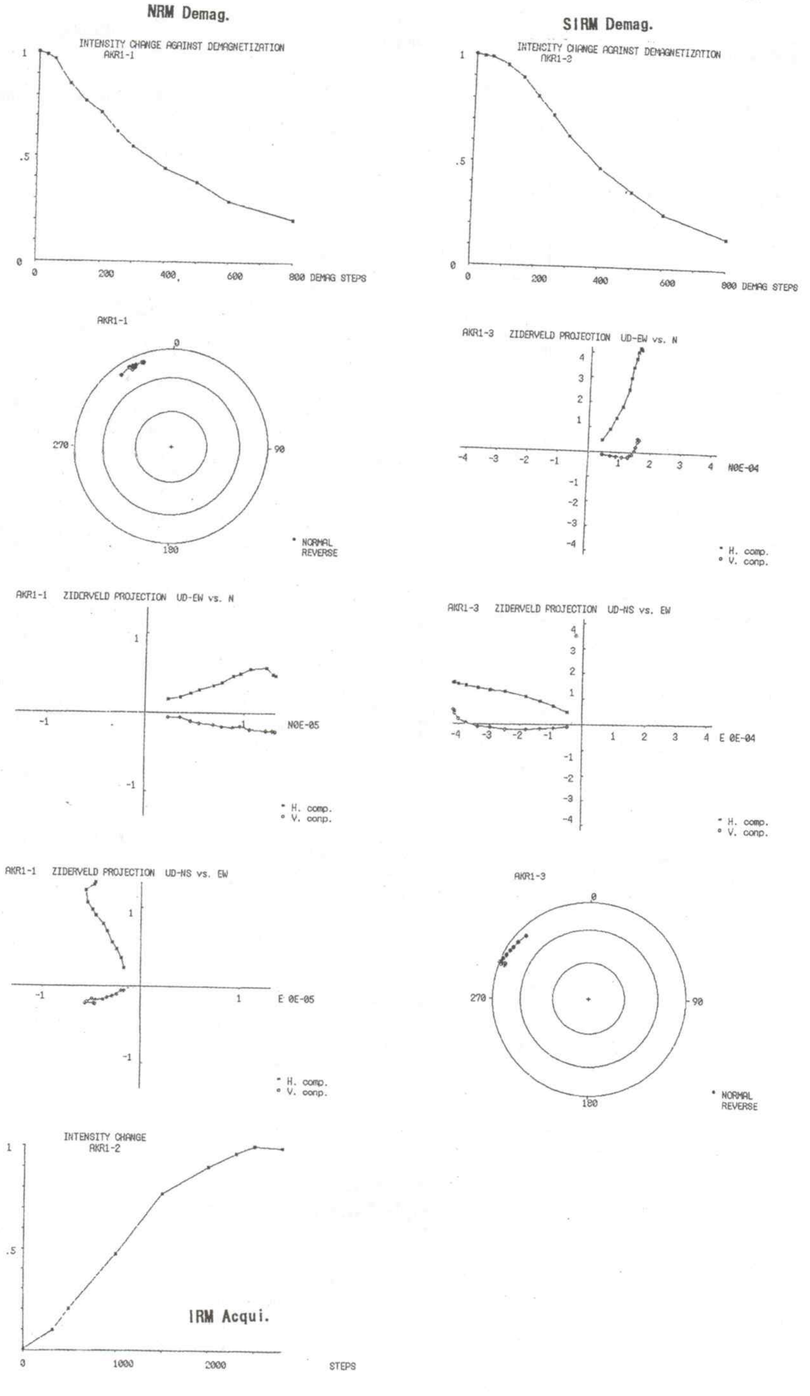

Fig.3-2.
Sample No.14

No.30 Kagoshima □

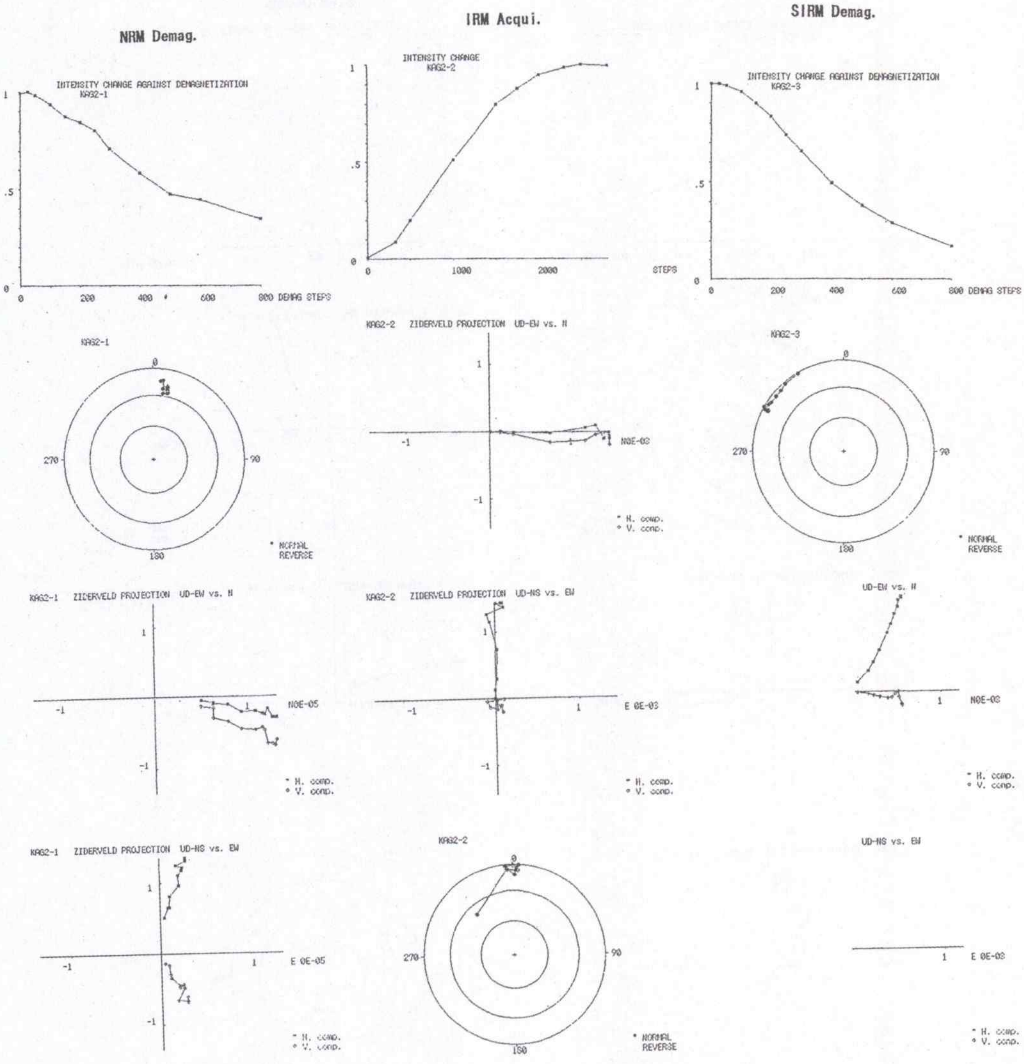

Fig.3-3.
Sample No.30

No.42 Matsumoto ○

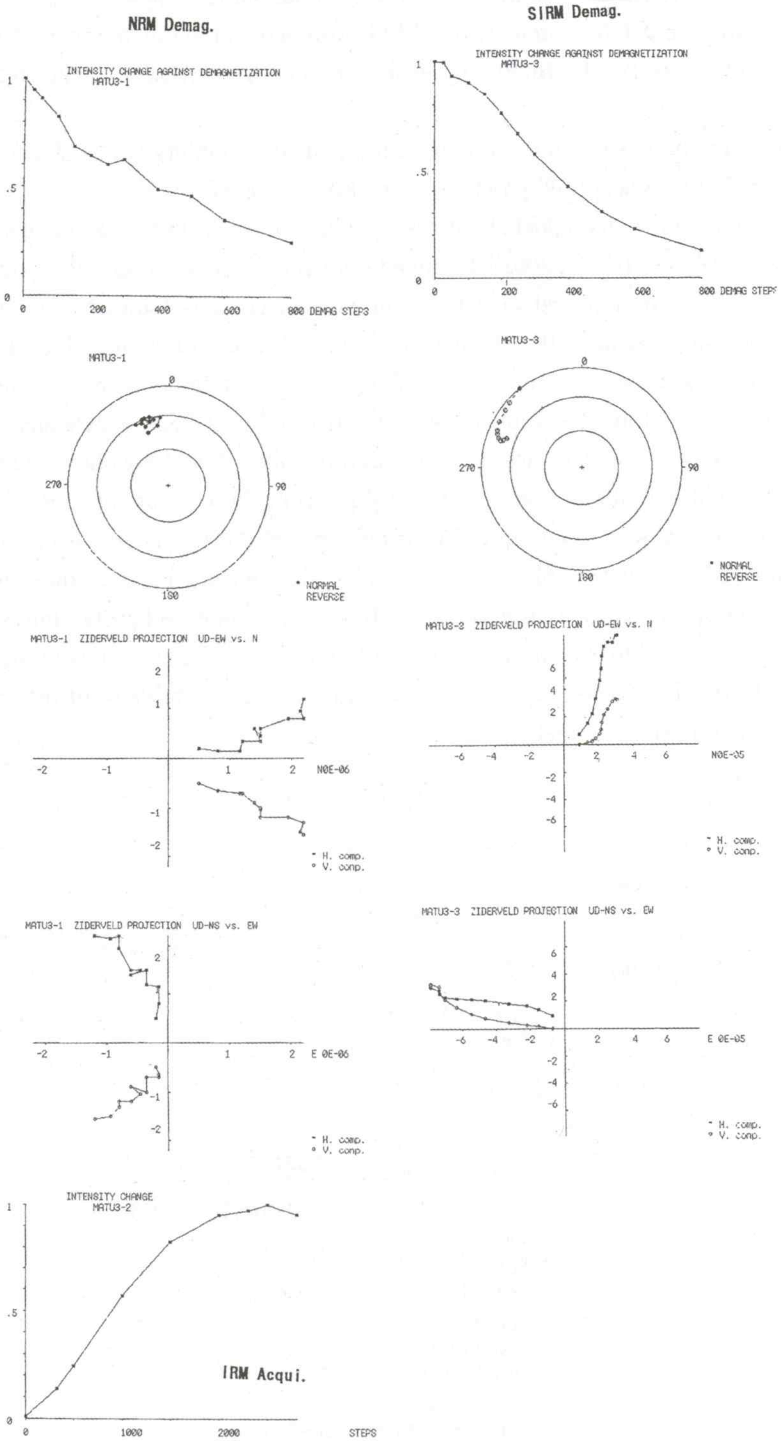

Fig.3-4.
Sample No.42

(2) SIRM and Susceptibility: Examples of AF demagnetization and Zijderbelt diagram for the SIRM are shown in Fig.3. MDF of SIRM is about 30mT, almost the same as that of NRM. As shown in Fig.4, the intensity of NRM is proportional to the intensity of SIRM.

Susceptibility measured by Birtington system ranges from $0.1 \times 10^{-8} m^3/kg$ to $26.9 \times 10^{-8} m^3/kg$.

SIRM intensity increases proportionally with initial susceptibility (χ) as shown in Fig.5. The ratio of SIRM to susceptibility ranges from 5kA/m to 20kA/m.

According to the previous report about susceptibility on roads, two peaks of susceptibility were found in one lane (Ueno, 2002). In the additional researches to find the origin of the high susceptibility, the exhaust dust from the vent of car was found to have the high susceptibility (Nakai et al, 2005). Vent which is fixed near either one side of the tire, scatters the dust with high susceptibility making two susceptibility peaks in one lane on the road. At the same time, the vent scatters the dust to the air. Leaves of azalea with thin hair on both side of the surface are sticky enough to collect the atmospheric dust. As the result, attachment and absorption of exhaust dust from the vent of car increases initial susceptibility of leaves of azalea in the crowded city where traffic jam is an every day affair. High NRM and susceptibility near the rail station is considered as the same. Iron-containing dust produced by friction between the rail and the wheel at the time when the train stops, is scattered to the air and absorbed to the leaves. The varieties of intensity of NRM and SIRM might reflect the amount and grain size assemblage of the magnetic minerals in the atmospheric dust.

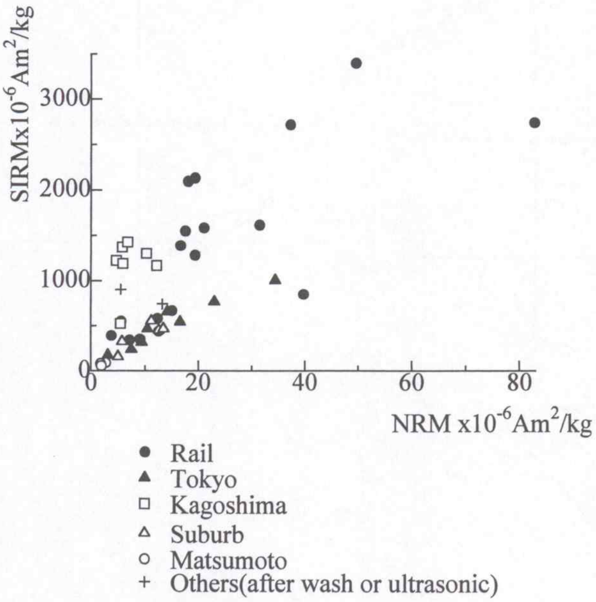

Fig.4.
Correlation of NRM with SIRM

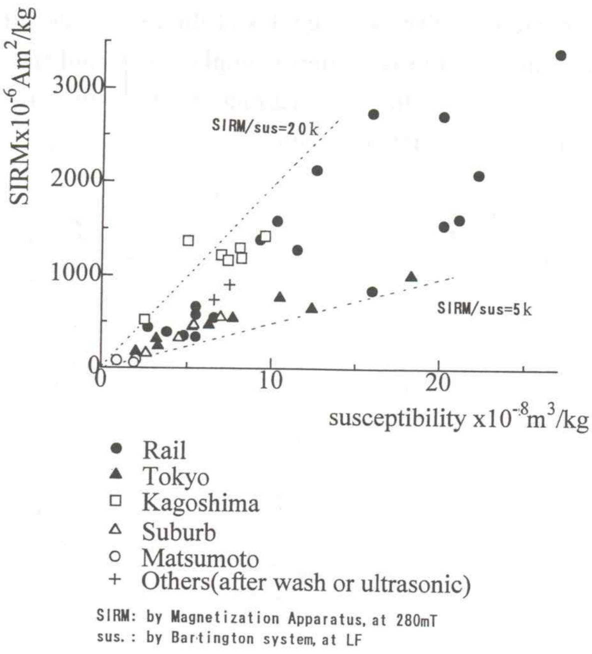

Fig.5.
Correlation of SIRM with susceptibility

(3) IRM: IRM intensity increases proportionally with the applied maximum AF up to about 150 mT, and saturated at about 250-300 mT as shown in Fig.3. AF demagnetization was performed by a method modified from Lowrie test (Lowrie, 1990), in which three components were acquired for 1.547T, 0,444T and 0,112T field intensity applied orthogonally (Fig.6).

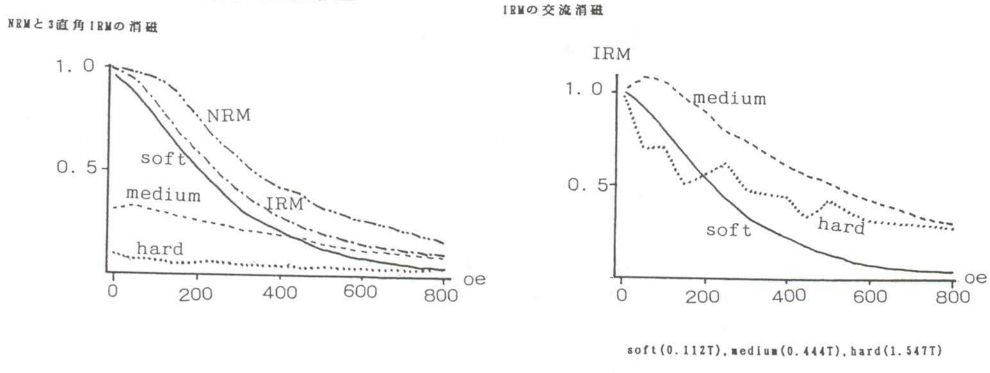

Fig.6.
Modified Lowrie test

(4) Hysteresis parameters: Typical examples of the hysteresis curves are shown in Fig.7. One is from near the railway station (sample No.1), and the other is from the suburbs (sample No.38). Fig.8 is the Day diagram, in which all of the three data fall in pseudo single domain range of titano-magnetite.

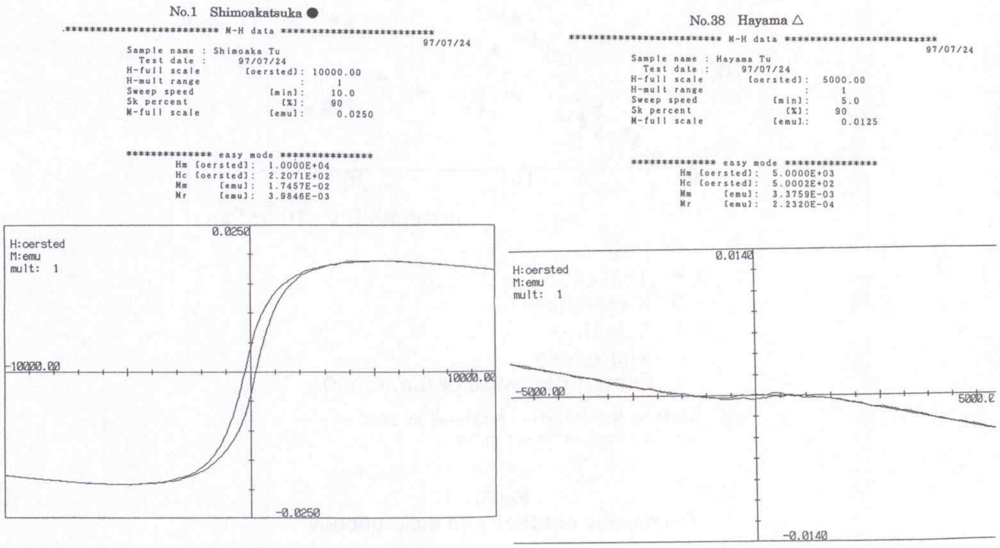

Fig.7.
Examples of the hysteresis curves

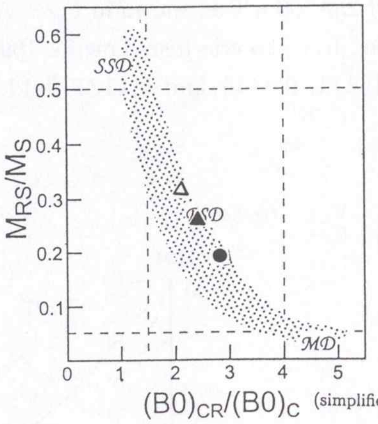

(simplified after Day *et al.*, 1977)

	Jrs/Js	Hc mT	Hcr mT
●No. 1	0. 22	22	66
▲No. 24	0. 25	15	39
△No. 35	0. 30	14	33

Fig.8.
Day diagram

(5) X-ray diffraction analysis and SEM-EDX (Scanning Electron Microscope-Energy Dispersive X-ray Analyzer) analysis, and wet chemical analysis: They were carried at RIKEN by Dr. S. Yabuki and Mr. Y. Iinuma. Sample No.2 was prepared for the analysis.

(5)-1 X-ray diffraction analysis of total leaves after dried for one week at 60℃ and powdered (Fe=0.13%)was carried. Amorphous carbon is dominant. Compound of Fe could not be found. Whewellite[C_2CaO_4,H_2O] and Polihalte[$K_2Ca_2Mg(SO_4)_4$, $2H_2O$],which are familiar in plants are identified(Fig.9). Enrichment of magnetic portion is required for the better analysis.

(5)-2 X-ray diffraction analysis of magnetic powder (attractive to magnet) was carried. In Fig.10, result of the powder under 180μm is shown. New candidates of Fe-compound are revealed. Matching result of Fig.10 is shown in Fig.11.Calcium Iron Magnesium Carbonate [Ankerite ($Ca(FeMg)(CO_3)_2$)] becomes the candidates. Calcium Magnesium Carbonate [Calcite Magnesian ($(CaMg)CO_3$)] is also found. Reliability of the matching is in Table 2. Reliability of matching for the Ankerite is low.

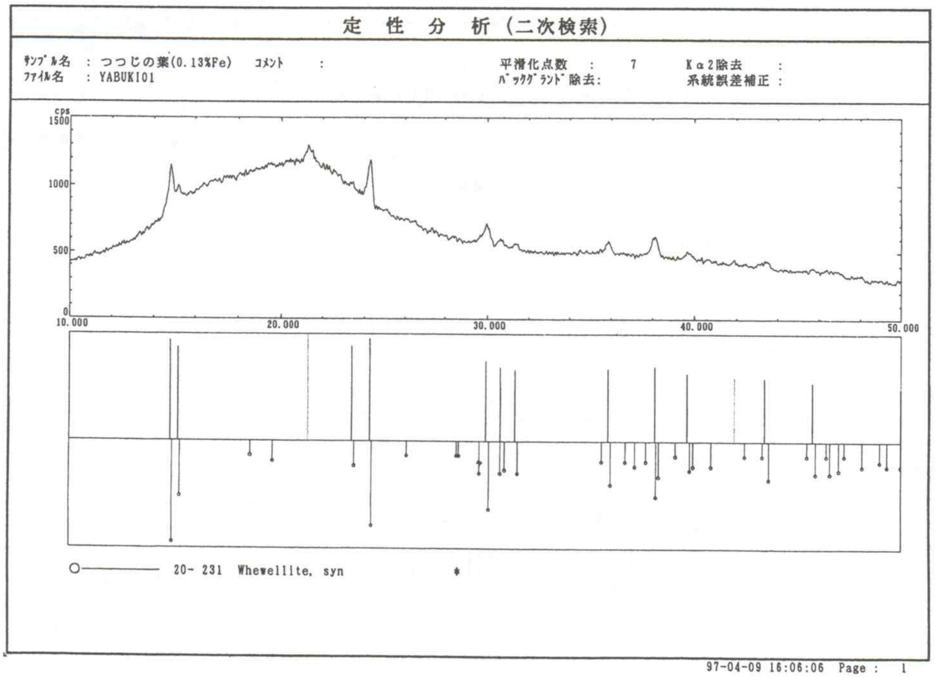

Fig.9.
X-ray diffraction analysis of total leaves

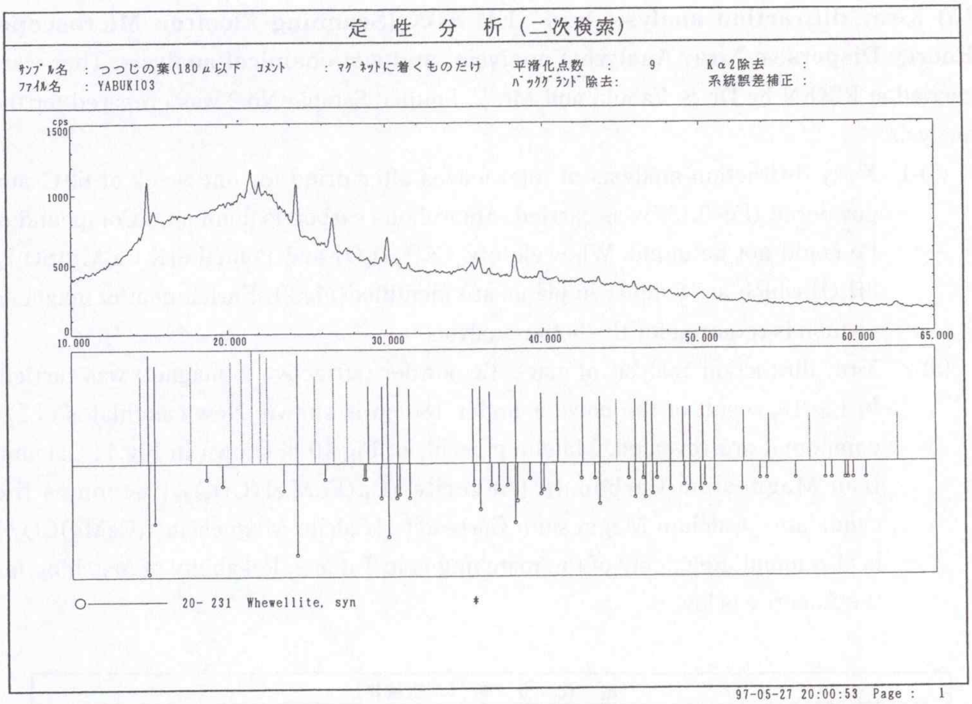

Fig.10.
X-ray diffraction analysis of magnetic portion

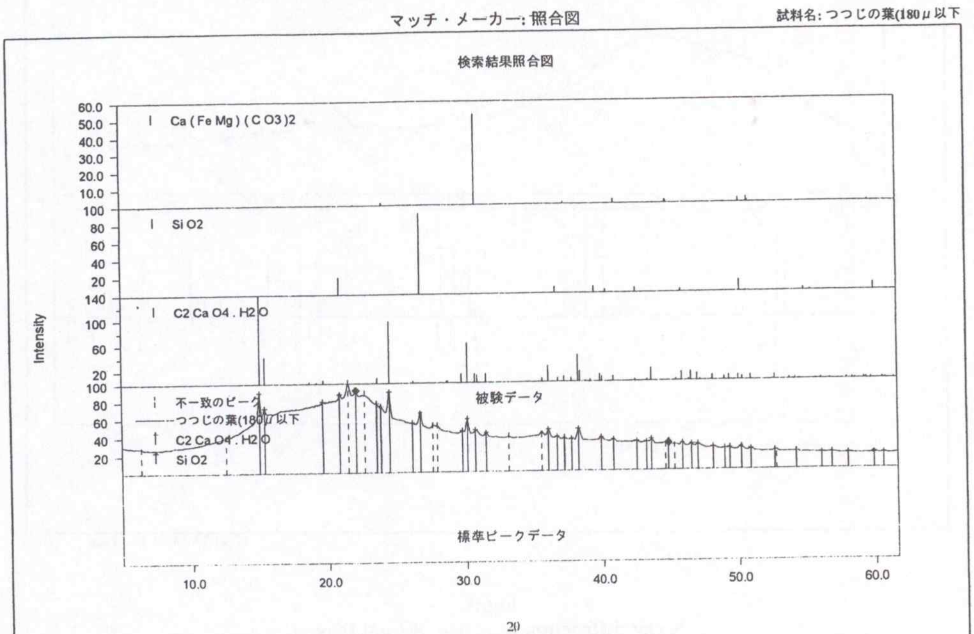

Fig.11.
Matching result in X-ray diffraction analysis of magnetic portion

(5)-3 Fe content by wet chemical analysis

Fe content of the dried powder is 0.13%, and of natural leaves is 0.053% (Table3)

(5)-4 Elemental analysis by SEM-EDX.

SEM-EDX analysis was carried for the particles in which Fe was included as the main element. Examples are shown in Fig.12. Particles containing Fe oxide, metallic Fe and Fe included in silicate are identified qualitatively. Aluminum-silicate, Magnesium-silicate and organic elements are identified for the others.

(6) Mössbouer effects: Mössbauer effects analysis was carried for the same magnetic sample as used for X-ray diffraction analysis ((5)-2) and SEM-EDX analysis ((5)-4), at laboratory of Prof. H. Ino, Faculty of Engineering, Tokyo University. Fig. 13 is the result. β-FeO(OH) and γ-FeO(OH) are suggested to the main magnetic minerals from the Doppler velocity. For comparison, compiled Doppler velocity of the magnetic mineral is listed in Table 4 (copied from The Chemical Society of Japan, 1993).

マッチ・メーカー: 登録された結晶相　　試料名: つつじの葉(180μ以下

登録物質のリスト

	PDF No.	信頼度	量比	物質名
A:	20-0231	18.26%		Calcium Oxalate Hydrate / Whewellite, Syn (C2 Ca O4 . H2 O)
B:	33-1161	13.22%		Silicon Oxide / Quartz, Syn (Si O2)
C:	41-0586	3.193%		Calcium Iron Magnesium Carbonate / Ankerite (Ca (Fe Mg) (C O3)2)
D:	43-0697	2.299%		Calcium Magnesium Carbonate / Calcite, Magnesian ((Ca Mg) C O3)

信頼度計算の詳細表示

	A	B	C	D
信頼度:	18.26	13.22	3.19	2.30
被験ピークの一致率:	35/67	13/67	7/67	6/67
(%):	52.24	19.40	10.45	8.96
標準ピークの一致率:	35/55	13/20	7/12	6/24
(%):	63.64	65.00	58.33	25.00
ピーク位置の一致率:	78.43	82.16	56.14	83.39
強度の一致率:	91.36	93.57	93.89	96.77
指定化学元素の一致率:	100.00	100.00	100.00	100.00

Table 2.
Reliability of matches in X-ray diffraction analysis

Wet chemical analysis (6NHCL, ICP)

Fe content: dried	**(1week at 60°C)**	**0.13%**
natural	**(calculated)**	**0.053%**

Table 3.
Fe content by wet chemical analysis

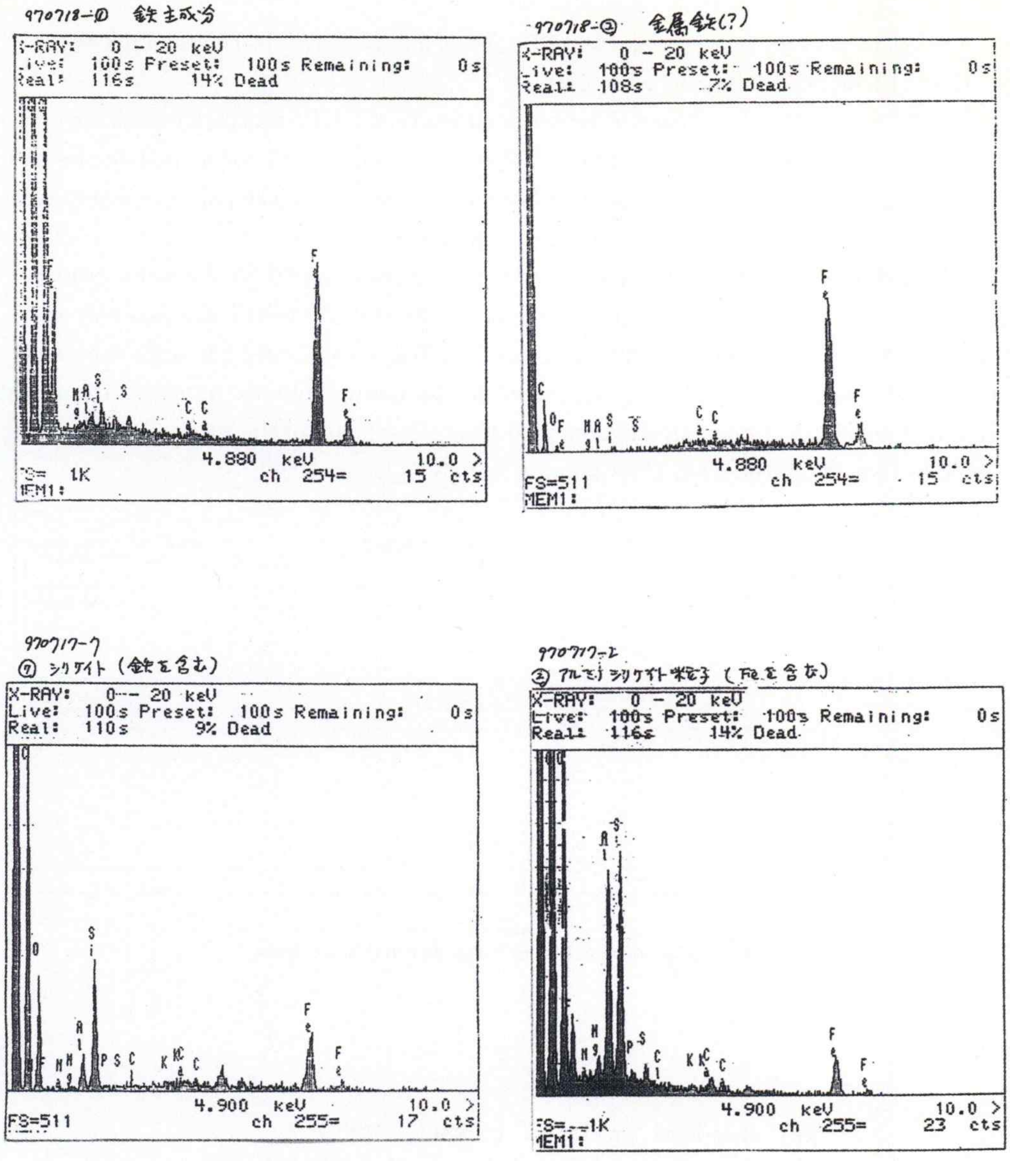

Fig.12.
Typical examples in SEM-EDX analysis

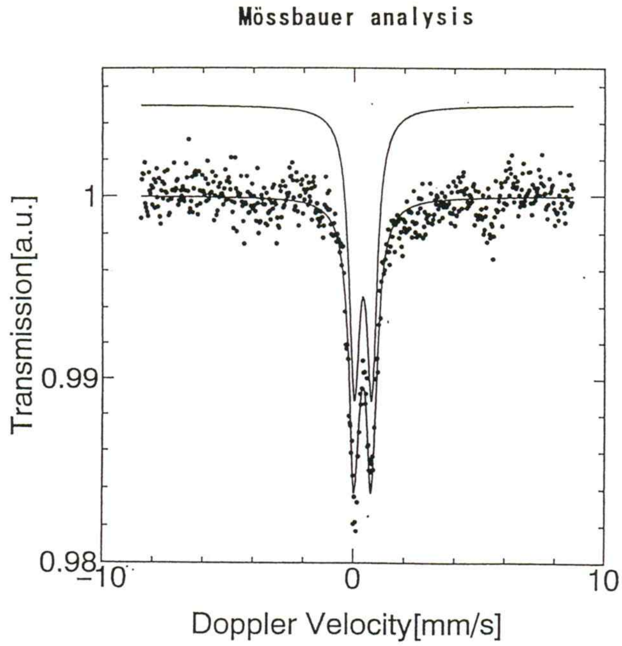

IS (= δ) 0. 36+0. 01 mm/s
QS (= ΔE_Q) 0. 68+0. 01 mm/s
B_{hf} 0. 51+0. 01 mm/s

Fig.13.
Mössbouer effect analysis

表 14・158 種々の ^{57}Fe 化合物のメスバウアーパラメーター

物質	T/K	δ/mm s^{-1}	ΔE_Q/mm s^{-1}	H/T
α-Fe	室温 He	0 +0.12		33.0
310 ステンレス鋼	室温	−0.09		0
FeF_2	298 4.2	+1.37 +1.48	2.79 2.85	0 0
$FeCl_2$	78 4.2	+1.097 +1.093	0.895 1.210	0 0.4
$FeCl_2 \cdot 2H_2O$	298	+1.03	2.50	0
$FeCl_2 \cdot 4H_2O$	室温	+1.221	2.984	0
$FeSO_4$	室温 4.2	+1.270	2.726 3.89	0 18.5
$[Fe(H_2O)_6]SO_4 \cdot H_2O$	室温 5	+1.261 +1.391	+3.217 +3.384	0 .0
FeF_3	296.5 4.2	+0.489	 0.044	0 61.8
$FeCl_3$	室温 4.2	+0.436 +0.461	 0.04	0 44.5

物質	T/K	δ/mm s^{-1}	ΔE_Q/mm s^{-1}	H/T
$FeCl_3 \cdot 6H_2O$	78	+0.60	0.91	0
$K_4[Fe(CN)_6]$	143	+0.04		0
$K_3[Fe(CN)_6]$	298 0.04	−0.124	0.280	0 19.3
$Na_2[Fe(CN)_5NO] \cdot 2H_2O$	298	−0.258	+1.705	0
$K_3[Fe(C_2O_4)_3]$	室温	+0.33		0
$Fe(CO)_5$	80	−0.09	2.57	0
$Fe_3(CO)_{12}$	80	+0.05 +0.11	0.13 1.13	0 0
フェロセン	室温	+0.53	2.37	0
α-Fe_2O_3	室温 He	+0.36 +0.46	−0.4 +0.80	51.7 54.4
γ-Fe_2O_3	室温 77	+0.27 +0.41		48.8 49.9 50.8 52.5

物質	T/K	δ/mm s^{-1}	ΔE_Q/mm s^{-1}	H/T
Fe_3O_4	300			49.1 45.3
α-FeOOH	291 He	+0.35		38.4 50.4
β-FeOOH	室温 He	+0.38	0.7	0 47.5
γ-FeOOH	室温 He	+0.30	0.55	0 46
$FeTiO_3$	室温 He	+1.02 +1.23	0.65 +1.42	0 4.5
$NiFe_2O_4$	室温			50.6 54.8
$SrFeO_3$	298 He	+0.054 +0.146		0 33.1
ヘモグロビン	195 4	0.90 0.91	2.40 2.40	
酸素ヘモグロビン	195 1.2	0.20 0.24	1.89 2.24	

Table 4.
Compiled Doppler velocity of magnetic minerals in Mössbouer effect
(copied from The Chemical Society of Japan,1993)

(7) Microscopic observation:

(7)-1 Electric-microscopic observation was performed by Prof. J. Akai, Faculty of Science, Niigata University. Magnetic powder (attractive to magnet) under 250 μm after dried for one week at 60℃ was used. As shown in Fig.14, magnetic mineral could not be found in this study.

(7)-2 Microscopic observation after ashed by plasma inorganizer was carried assisted by Ms. M. Shimizu at Natural Science Laboratory, Toyo University. Opaque minerals of few micro-meter to 100 micro-meter could be seen as shown in Fig.15.

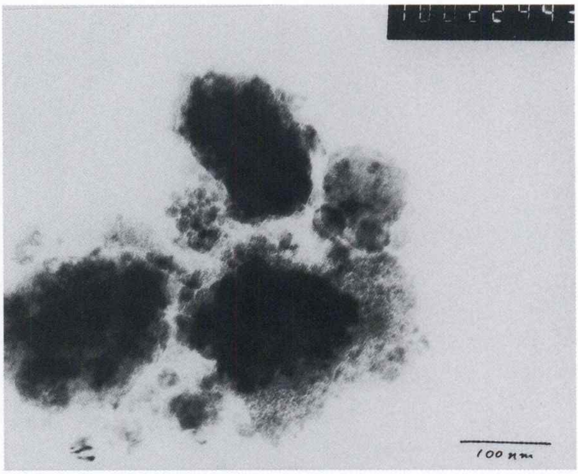

Fig.14.
Electric-microscopic observation

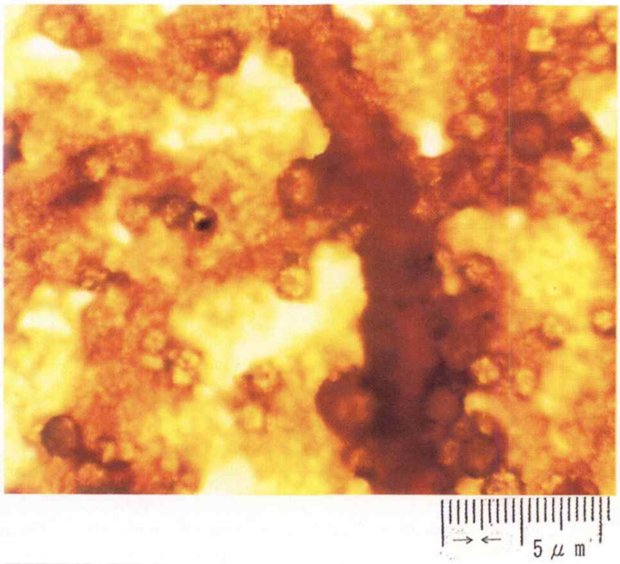

Fig.15.
Microscopic observation after ashed

4. Discussions and conclusions

Intensities of NRM, SIRM and susceptibility are the highest near the railway station. Also, they are larger in the center of Tokyo than in the suburbs. The reason of high intensity near the railway station and in the center of Tokyo is as follows. Iron-containing powder produced by friction between the rail and the wheel when the train stops, or iron-containing powder discharged from the vent of cars, spreads to the air and attaches to the leaves. Leaves of azalea have cilia and are sticky enough to catch and keep and absorb the iron-containing powder in the air.

Natural remanent magnetism reflects the direction of the earth's magnetic field, which suggests the quick orientation of magnetism has occurred after attachment of powder to the leaves. This idea of quick orientation seems useful to consider the process of acquisition of DRM (Detrial Remanent Magnetizm).

As to the magnetic mineral, rock magnetic experiments such as AC demagnetization curves and hysteresis parameters suggest that the main magnetic mineral is psudo-single domain magnetite. In X-ray diffraction analysis of magnetic powder (attractive to magnet) under 180μm , Ankerite $Ca(FeMg)(CO_3)_2$ is suggested as the Fe containing compound with the low reliability. In SEM-EDX analyses, particles of Fe oxide, metallic Fe and Fe included in silicate are identified qualitatively. In the Mössbauer effect analysis, magnetite could not be found and β-FeO(OH) and γ-FeO(OH) are suggested to the main magnetic minerals.

Acknowledgements

The author is grateful for cooperation to obtain data of the NRM and SIRM to Dr. Minoru Funaki of NIPR (National Institute of Polar Research), SEM-EDX analyses and wet chemical analysis of Fe to Dr. Sadayo Yabuki and Mr. Yasuhiro Iimura of RIKEN(The Institute of Physical and Chemical Research), electro-microscopic observation to Prof. Junji Akai of Niigata Univ., Mössbauer analyses to Prof. Hiromitsu Ino of Tokyo Univ. and ashed leaves observation to Ms. Mitsuko Shimizu of Toyo Univ.

References

Day, R., Fuller,M.D. & Schmidt,V.A. (1977) Hysteresis properties of titanomagnetites: grain size and composition dependence. Phys. Earth Planet Inter. 13, 260-266.

Lowrie, W. (1990) Identification of ferromagnetic minerals in a rock by coercivity and unblocking temperature properties. Geophys. Res. Lett. 17, 159-162.

Nakai,M., Ueno.N., Tazaki,K. Watanabe,H., Asada,R. and Shimazaki,H.(2005) Origin of the pollution characterized by high susceptibility-Magnetic character of the exhaust dust from the vent of bus. IAGA-2005-A-01206, GAI12 (Toulouse).

The Chemical Society of Japan (1993). 改訂 4 版化学便覧 Maruzen(written in Japanese) ISBN4-621-03870-2 C3043 Ⅱ-648.

Ueno, N. (1993) Natural remanent magnetization of plants (1).(written in Japanese) Journal of the Toyo Univ., General Education (Natural Sci.), 37, 1-8.

Ueno, N. (1996) Magnetic characters of plants (2).(written in Japanese) Journal of the Toyo Univ., General Education (Natural Sci.), 40, 43-48.

Ueno, N. (1997) Magnetism of leaves of azalea: Abstracts IAGA-1997(Uppsala) Session 1.18 p107.

Ueno, N. (2002) Susceptibility measurement to detect pollution by traffic on paved roads: Journal of the Toyo Univ., Natural Sci., 46, 43-52.

Zijderveld, J.D.A.(1975) Paleomagnetism of the Esterel rocks. Doctoral thesis, Univ. of Utrecht,199 pp.

要　旨

上野直子：つつじの葉の磁性―磁性の特徴および環境との関連

つつじの葉は日本中に街路樹として広く植えられている．葉は繊毛で覆われ，手で触ると粘性があることに気付く．著者は種々の植物について自然に持つ磁性強度を測定したが，最も強度が大きいのは，つつじの葉であった．そこで，つつじの葉の磁性特性を調査するため岩石磁気の手法での解析，X 線解析，メスバワー解析，顕微鏡解析を試みた．葉の磁性の特徴を明らかにすることによって，採取地点による差が環境の指標になることを期待した．実験は，船木實博士（極地研），矢吹貞代博士・飯村康紘氏（理研），井野博満教授（東大工），赤井純治教授（新潟大理），清水満子氏（東洋大）のご協力により行われた．（所属は実験当時）

岩石磁気の手法での解析：NRM 強度は最高で 83×10^{-6} Am^2/kg，最低で 2×10^{-6} Am^2/kg である．鉄道の駅近くと東京の中心部で強く，採取地域による差がでた．高強度の原因は，駅では停車時のブレーキによる車輪と線路の摩擦で鉄粉が空気中に広がる．道路際では車の排気ガスに含まれる磁性物質（中井他，2005）が空気中に広がる．車両通行量の多い都心では，空中の磁性物質も多い．空気中の磁性物質が多いと繊毛と粘性のあるつつじの葉に付着する量も多い．また葉の磁性の向きは地球磁場方向である．このことから磁性は付着とほぼ同時に地球磁場方向に揃うと考えられる．短時間内で粒子の磁性が地球磁場方向に揃うという考え方は，堆積物の残留磁化の獲得過程を考える上で重要である．

SIRM 強度は NRM 強度に比例するが，比例定数には地域差が見られる．3 軸分離による IRM の獲得曲線を 1 試料について測定した．

初期帯磁率は SIRM 強度に比例する．比例定数には地域差が見られる．

代表的試料の**ヒステリシス**から得られたパラメーターはチタノマグネタイトの擬似単磁区構造領域にプロットされる．

X 線解析：試料番号 No.2 についてのみ行った．磁石に付く 180μm 以下の粒子の X 線回析では，信頼性は低いが Ankerite（$Ca(FeMg)(CO_3)_2$）が鉄を含む化合物の候補となった．SEM-EDX による Fe を主成分とする粒子の元素分析では．定性的であるが，鉄酸化物，金属鉄，鉄を含むシリケイト粒子，鉄を含むアルミノシリケイト粒子，鉄を含むマグネシウムシリケイト粒子が見られる．

メスバワー解析：試料番号 No.2 についてのみ行った．異性体シフトと四極子分裂のパラメーターからは Fe 化合物のなかでオキシ水酸化鉄（β-FeO(OH)，γ-FeO(OH)）が最適となり，マグネタイトに対応するピークは見えなかった．

今回の**顕微鏡解析**では特記する結果は得られなかった．

以上のことからつつじの葉には，鉄の化合物が付着しており，これが残留磁化の原因となり，空気汚染と関連することがわかった．ただし，化合物は水酸化鉄や Ankerite など候補はあるものの特定できなかった．